Influence of sulphate ions on the crystal chemistry of white cement mortars with a high content of marble filler powder

Influence of sulphate ions on the crystal chemistry of white cement mortars with a high content of marble filler powder

V A Stoyanov[1,2]*, V Petkova[3], B Kostova[4]

[1] Department of Technology and Construction Management, Faculty of Construction, USEA (VSU) "L. Karavelov", 175 Suhodolska St., 1373 Sofia, Bulgaria;
[2] Academy of the Ministry of Interior, Department of Safety and Prevention, 17 Pirotska Str., 1309 Sofia, Bulgaria
[3] Institute of Mineralogy and Crystallography "Acad. Ivan Kostov", Bulgarian Academy of Sciences, Acad. Georgi Bonchev Str., Block 107, 1113, Sofia, Bulgaria;
[4] Department of Natural Sciences, New Bulgarian University, 21 Montevideo St., 1618 Sofia, Bulgaria

* E-mail: vensy.stoyanov@vsu.bg

Abstract. Objects of this research are white cement mortars, characterized by both of high content of addition of marble powder and reduced water-cement ratio. The hardened cement mortars, formed after 28-and 120-day curing under standard conditions, are studied. The newly formed phases, containing $[SO_4]^{2-}$, $[CO_3]^{2-}$, $[OH]^-$, etc., are identified using X-ray powder diffraction, infrared spectroscopy and thermal analysis (coupled with analysis of the outgoing gas mixture by mass spectrometry). Based on of the formed calcium silicate hydrates, calcium aluminate hydrates, the influence of sulphate ions is analysed and the mechanism of the thermal decomposition reaction at high temperatures in an oxidizing gas environment is studied. This allows us to establish that the hydration of Portland cement depends on the addition of marble powder (technically calcium carbonate $CaCO_3$), as well as mono- and hemicarboaluminates are formed instead of monosulphoaluminates.

1. Introduction

Modern building materials have a low footprint on the environment and lower energy costs for their production [1, 2, 3]. One of the main directions for their production is the replacement of some of their components with recycled materials, as this effect is most significant for the expensive and polluting production of cement, mortar and concrete [4, 5]. Limestone quarry waste is often used as inert additives and aggregates for the production of cement-based mortars, but this component increases the content of sulphate and carbonate ions in cement mortars. Knowledge of the microstructure and crystal chemistry of such mortars is important to achieve good performance indicators and durability [6].

The aim of this work was to study the amounts of new formed solid phases with $[SO_4]^{2-}$, $[CO_3]^{2-}$, $[OH]^-$, formed at different curing times of mortars based on white Portland cement. Mortars with a high content of inert mineral aggregate (marble powder) and a low water-to-cement ratio were studied. The phase composition was examined by powder X-ray diffraction (PXRD), Fourier transform infrared spectroscopy (FTIR) and thermal analysis (TG/DTG-DSC).

2. Materials and methods

2.1. Components

The samples were prepared with white Portland cement CEM I 52.5 N (produced by Devnya Cement; Bulgaria), aggregate - marble powder type (produced by White Marble Products AIAS SA; Greece), polycarboxylate-based high range water reducer (HRWR - Sika ViscoCrete 5-800) and distilled water. The chemical admixture was chloride-free, soluble in water, without any retarding effects and with a density of 1.07 g/cm^3 (at 20°C).

The chemical composition of white Portland cement was (in wt%): SiO_2 – 24.3; Al_2O_3 – 2.1; Fe_2O_3 – 0.2; CaO – 68.3; MgO – 0.3; Na_2O – 0.13; K_2O – 0.02; Free lime – 1.9. Thus, the mineral composition, calculated by Bogue method was (in wt%): C_3S – 72.13; C_2S – 15.28; C_3A – 5.23; C_4AF – 0.61. The chemical composition of marble powder (in wt. %) was: $CO_2 + H_2O$ – 45.7; SiO_2 – 0.12; Al_2O_3 – 0.38; Fe_2O_3 – 0.14; CaO – 32.9; MgO – 20.0; Na_2O – 0.05; K_2O – 0.19; MnO – 0.01. The decarbonization at 1000°C of this aggregate was divided to two stages (DTA peaks – 806.6°C and 821.2°C) with total mass loses of about 45% and, thus the mineral composition is defined as dolomite and Mg-rich calcite. The polydispersity of the aggregate was determined by the following parameters: the maximal size of grains – 2 mm; grains with sizes < 0.125 mm – 50.0 wt % and grains with sizes < 0.063 mm – 35.0 wt %.

2.2. Samples preparation

The sample composition was characterized by the following ratios:

- cement-to-aggregate ratio – 1:2 (in mass parts);
- water-to-cement ratio – 0.40;
- dosage of HRWR – 2.0% by the weight of white cement.

Based on these data the water-to-fines mass ratio was 0.235, where fines were all particles with sizes below 125 μm. After the procedure of mixing, based on EN 196-1:2016, the samples were moulded without any compacting treatment in 6 prisms (two prisms for each sample), 40×40×160 mm, for 1 day in a moist atmosphere (> 95% RH and 20°C) [7]. After the samples were stored under water (20ºC) until strength testing (1, 3, 7, 14, 28 and 120 days). The names of the samples were based on the ageing time of the samples – C001, C003, C007, C014, C028 and C120, respectively.

2.3. Experimental Methods

The density and adsorption after immersion were measured according to ASTM C642-13 [8]. Due to the different densities of the samples, the values of adsorption were adjusted to comparable values. The compressive strengths at 28 and 120 days of water curing samples were measured according to EN 196-1:2016 [7].

To measure the porosity of broken parts samples with a mass of 2.0±0.3 mg were analysed by mercury intrusion porosimetry method using Carlo Erba, Porosimeter Mod. 1520 (pressure range 1-150 atm corresponding to pore size range 50-15000 nm. The PXRD patterns were performed on X-Ray powder diffractometer D2 Phaser BrukerAXS, CuKα radiation (λ = 0.15418 nm) (operating at 30 kV, 10 mA) from 5 to 80 °2θ with a step of 0.05° (1.0±0.1 mg grinded sample; particle sizes below 0.075 mm). FTIR measurements were performed by FT-IR Spectrometer, Varian 660-IR, Austria, 2009, covering the range of 400-4000 cm^{-1}, KBr tabletting. TG/DTG-DSC analyses were carried out on a Setsys Evolution 2400, SETARAM, France, combined with an OmniStar mass-spectrometer (heating rate of 10°C.min^{-1}). The operational characteristics of the TG/DTG–DSC- system were: sample mass of 18.0±2.0 mg; ceramic sample crucible and static air atmosphere.

3. Results and Analysis

3.1. PXRD phase analysis

Based on PXRD phase analysis several phases were identified (table 1). They can be divided into the following two groups of minerals:

- relict minerals from the raw composition: belite, albite, anorthite, Mg-rich calcite, quartz, dolomite;
- newly formed minerals: portlandite, ettringite, mono- and hemicarboaluminate, scolecite, hillebrandite, nonotlite, spurrite, artinite and $Ca(HSO_4)_2$.

Table 1. Results from PXRD analysis.

No	Description	Sample	Identified phases
1	Non-hydrated relict cement phases	C001, C003, C007, C014, C028, C120	Belite (C_2S), 49-1673 – $2CaO.SiO_2$
			Alite (C_3S), 11-0593 – $(Na,Ca)Al(Si,Al)_3O_8$
			Anorthite (CAS_2), 41-1486 – $CaO.Al_2O_3.2SiO_2$
2	Non-hydrated phases relict of aggregate phases	C001, C003, C007, C014, C028, C120	Dolomite, 36-0426 – $CaCO_3.MgCO_3$ Mg-rich Calcite, 47-1743 – $CaCO_3$
3	New formed C-S-H gel phases	C001, C003, C007, C014, C028, C120	Portlandite (CH), 44-1481 – $Ca(OH)_2$
3.1	containing OH^- and CO_3^{2-}	C120	Monocarboaluminate, 41-0219 – $Ca_4Al_2(OH)_{12}(CO_3).5H_2O$
		C028, C120	Hemicarboaluminate, 41-0221 – $Ca_4Al_2(OH)_{12}(OH)(CO_3)_{0.5}.4H_2O$
		C003, C007, C014, C028, C120	Artinite, 72-1320 – $Mg_2(CO_3)(OH)_2.3H_2O$
3.2	containing OH^- and SO_4^{2-}	C001, C003, C007, C014, C028, C120	Ettringite, 41-1451 – $6Ca(OH)_2.Al_2(SO_4)_3.26H_2O$ Gypsum, 21-0167 – $CaSO_4.2H_2O$
		C014, C028, C120	$Ca(HSO_4)_2$, 85-1271
3.3	hydrosilicates formed from main oxides: CaO, Al_2O_3, SiO_2	C001, C003, C007, C014, C028, C120	Hillebrandite, 29-0373, 42-0538 – $CaSiO_3.Ca(OH)_2$
		C120	Scolecite, 41-1355 – $CaO.Al_2O_3.3SiO_2.3H_2O$ $CaAl_2Si_3O_{10}.3H_2O$
		C028, C120	Xonotlite, 23-0125 – $5CaO.6SiO_2.Ca(OH)_2$ $Ca_5Si_6O_{17}.Ca(OH)_2$
4	Water-free non-hydrated newly formed phases	C007, C014, C028, C120	Spurrite, 13-0496 – $Ca_5(SiO_4)_2CO_3$

3.2. FTIR Spectroscopy

The spectra, obtained by FTIR spectroscopy demonstrate a wide variety of streaks and are evidence of the formation of multiple hydrate phases in the samples (figure 1). This occurs in three areas – 1750-1240 cm^{-1}, 1300-900 cm^{-1} and 800-400 cm^{-1} in which the overlap of the lines is strongly expressed. At these intervals, the vibrational fluctuations of the functional groups, which are essential for the identification of the cement hydration products, are displayed.

The analysis of the results obtained from the FTIR spectroscopy studies proves the vibration bands of the minerals formed by the hydration of the cement minerals. In the analysis, several groups of new-formed phases can be identified:

- phases, containing chemically bonded water $[OH]^-$;
- phases, containing carbonate ions $[CO_3]^{2-}$, structurally bonded water $[OH]^-$ and chemically bonded water (H_2O);
- phases, containing sulphate $[SO_4]^{2-}$ ions, structurally bonded water $[OH]^-$ and chemically bonded water (H_2O).

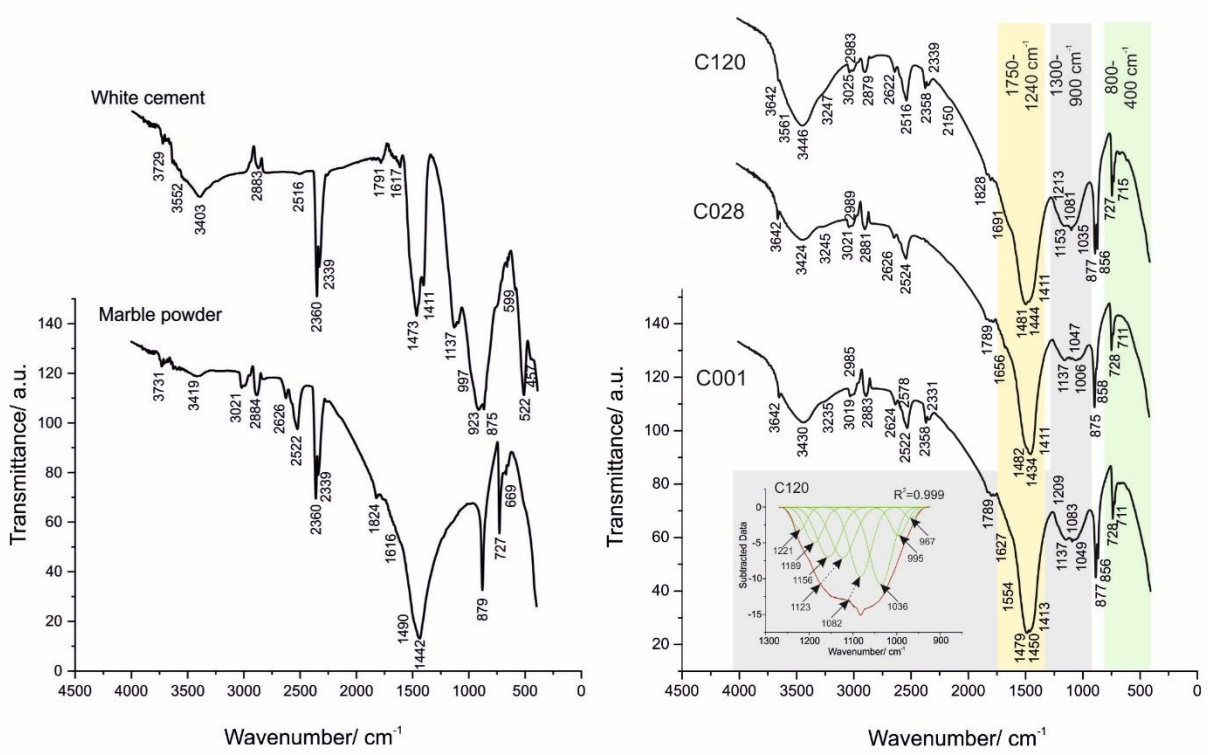

Figure 1. FTIR spectra of raw marble powder, white cement (left), C001, C028 and C120 (right). *Insertion:* peak decomposition via Gauss function within the range 900-1300 cm^{-1} of sample C120.

The analysis of the results obtained from the FTIR spectroscopy studies proves the vibration bands of the minerals formed by the hydration of the cement minerals. In the analysis, several groups of new-formed phases can be identified:

- phases, containing chemically bonded water $[OH]^-$;
- phases, containing carbonate ions $[CO_3]^{2-}$, structurally bonded water $[OH]^-$ and chemically bonded water (H_2O);
- phases, containing sulphate $[SO_4]^{2-}$ ions, structurally bonded water $[OH]^-$ and chemically bonded water (H_2O).

The components, used for the production of cement-based mortars, produce closely related new-formed hydrate phases, some of which are the same for all samples – portlandite, ettringite and hillebrandite. Mono/hemicarboaluminate and nonotlite were formed after 28 days, Scolecite - after 120 days of curing.

The results of the PXRD analysis and FTIR spectroscopy justify the chemical reactions during hydration of samples to be represented by the reactions forming the hydrate silicate phases, Mg-hydrogen carbonate and Ca-hydrogen sulphate phase, and water-free non-hydrated phases as spurrite. Compared to conventional mortars, prepared with quartz sand as fine aggregate, the use of marble powder increases the content of $[CO_3]^{2-}$-ions in cement mortars, leading to an isomorphic substitution of ettringite during hydration. These reactions can be described by the following equations:

$$3Ca^{2+} + HSiO_3^- + CO_3^{2-} + SO_4^{2-} + 5OH^- + 12H_2O \rightarrow 3Ca(OH)_2.Si(SO_4.CO_3).12H_2O \quad (1)$$

$$6Ca^{2+} + 2AlO_2^- + 3CO_3^{2-} + 3SO_4^{2-} + 6OH^- + 26H_2O \rightarrow 3Ca(OH)_2.3CaCO_3.Al_2(SO_4)_3.26H_2O \quad (2)$$

3.3. Thermal analysis

The data from the thermal analysis carried out on the solid components (white Portland cement and marble powder) is shown in figure 2, and the TG-DTG-DSC results for the tested cement compositions in figure 3. Some of the results are supplemented by the analysis of gas phases (figure 4). Processing of these data yields to obtaining both the thermal decomposition temperatures (it is assumed that this is the temperature in the inflexion point T_{infl}) and mass losses (ML), which are then arranged in tabular form (table 2).

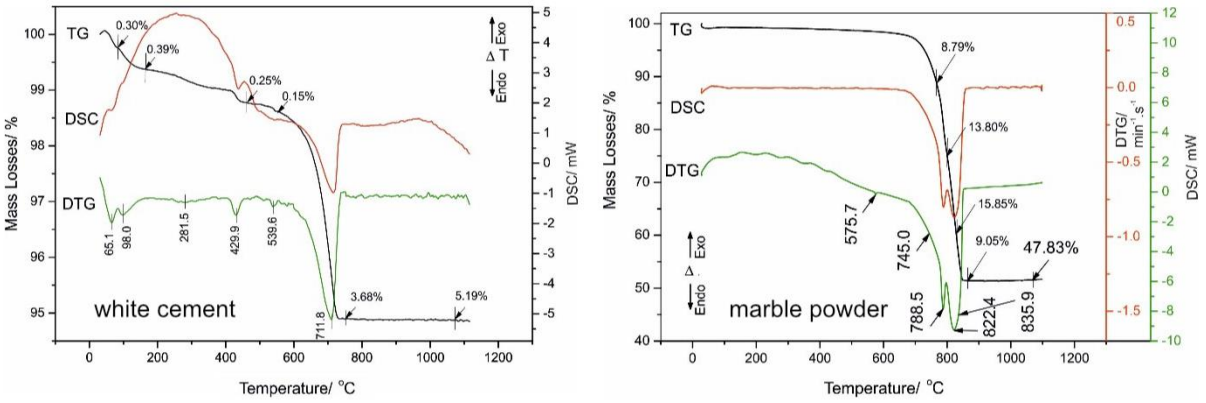

Figure 2. TG-DTG-DSC- curves of raw white cement (left) and raw marble powder (right).

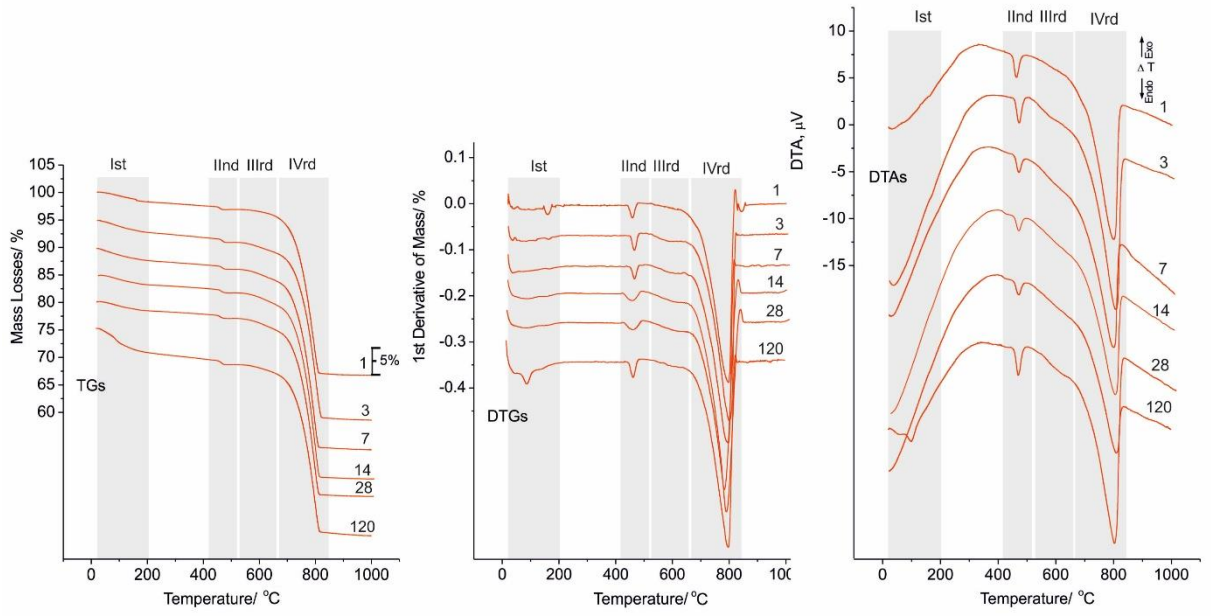

Figure 3. TG, DTA and DTG curves of samples C001-C120.

The mass losses are divided into four ranges: 1st range - 1.00-1.53%, 2nd range – 0.46-0.70%, 3rd – range 2.60-4.36% and 4th range – 3.30-30.10%. Such a distribution of mass losses is also related to four temperature intervals (stages) of samples' decomposition (table 2):

- 1st stage– dehydration (40-200°C);
- 2nd stage – dehydroxylation (420-470°C);
- 3rd stage – dehydroxylation, decarbonation and desulphurization (520-700°C);
- 4th stage– decarbonation and desulphurization (700-830°C).

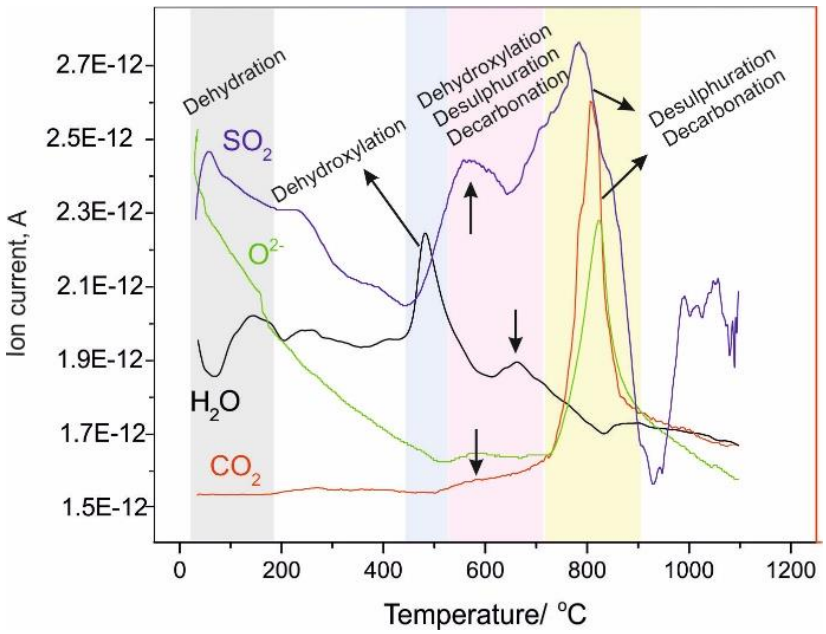

Figure 4. MS analysis of evolving gases of thermal decomposition of C120.

Table 2. Temperatures of thermal decomposition (T_{infl}) and mass losses (ML)

Sample	I stage 40-200℃ Dehydration		II stage 420-470℃ Dehydroxylation of $Ca(OH)_2$		III stage 520-700℃ Dehydroxylation of C-S-H		IV stage 700-830℃ Decarbonization of $[CO_3]^{2-}$ phases		Total mass losses, %
	T_{infl}, ℃	ML, %	T_{infl}, ℃	ML, %	T_{infl}, ℃	ML, %	T_{infl}, ℃	ML, %	
White cement	65.1 98.0	0.30 0.39	429.9	0.25	539.6	0.15	711.8	3.68	5.19
Marble powder	-	-	-	-	575.7	7.70	806.6	30.02	47.83
C001	84.8 161.1	1.67	459.5	0.57	609.3	0.84	795.8	29.02	33.30
C003	82.4 167.6	2.07	469.4	0.69	574.6	1.81	804.1	29.68	35.83
C007	169.7	2.17	470.8	0.69	589.8	2.40	786.4	29.45	35.94
C014	90.7 160.3	2.75	457.9	0.64	609.9	2.42	790.0	29.43	35.19
C028	135.3	0.76	426.7	1.23	566.5	0.94	721.5	28.98	34.38
C120	88.1 139.8	4.11	464.2	0.82	593.7	1.41	798.6	29.12	37.71

These four stages are referred to both the raw materials and the prepared mortars, taking into account differences in 3rd stage (dehydroxylation, decarbonation and desulphurization) as well as in 4th stage (decarbonation and desulphurization) [9, 10, 11]. In these two stages, the changes in the amount of crystal and bound water, decarbonation of carbonate and hydro-carbonate ions, as well as desulphurization of sulphate ions associated with the raw materials, their ratio and the resultant microstructures are defined. The detailed description of the mass losses (ML) and the related processes are as follows:

1st stage –an ongoing process of dehydration in the temperature range 40-200°C

In the low-temperature range up to 200°C, the crystal water is released from cement hydrate phases – gypsum and C-S-H gel. The results from PXRD analysis prove the existence of phases, forming gypsum and C-S-H gel (hydro-silicate minerals with fine structure, usually PXRD amorphous [9, 12]). The registered low ML are a result of their low amount in the samples – 0.76-4.11% (table 2).

2nd stage – an ongoing process of dehydroxylation in the temperature range 420-470°C

The thermal effects in this temperature range are weak, but well developed for all studied samples. Based on our previous research [9, 12, 13] and according to the other authors [10, 11, 14, 15], it can be assumed that the temperature dependences and ML at this stage are results from dehydroxylation of portlandite. The obtained lower ML (0.57-1.23%) is due to lower water-to-cement ratio as well as to water bonding in hydro-silicates, forming C-S-H gel. Despite the registered low ML, the dihydroxylation has been established by the decreasing of portlandite amount, namely decreasing crystal water in portlandite and increased amount of water included in C-S-H gel.

3rd stage – an ongoing process of dehydroxylation, decarbonation and desulphurization in the temperature range 520-700°C

The result of thermal analysis for this stage was supplemented by evolving gas analysis in the order to clarify and correct interpretation of the thermal decomposition reaction mechanism. A slight increase in ML up to 0.84% (C001) and 2.42% (C014) was measured, which can be explained by the incorporation of larger amounts of hydroxyl, carbonate and/or sulphate ions in these samples. Besides, in this temperature range, the dihydroxylation of bonded water in C-S-H gel minerals (ettringite, mono/polycarboaluminate, monosulphoaluminate, etc.) occur [10, 11, 14, 15, 16]. Decomposition processes in this temperature range are more complex and involve stages of overlapping thermal reactions in which hydroxyl, carbonate and/or sulphate ions are also released. This is defined by the mass spectrometric analysis of the evolving gases, which established that the dehydroxylation process is carried out parallel with decarbonization and desulphurization. The combined separation of carbonate and hydroxyl ions implies both their independent emission from the solid phase and the emission as hydroxycarbonate ions.

The ongoing reactions refer to dihydroxylation-decarbonation to release of carbonate ions from hydrogen-carbonate phases. For example, $CaHCO_3$ and monocarboaluminates, formed during the initial hydration of cement minerals [15], are metastable and they are decarbonated at temperatures, lower than that of calcite. This fact explains the inserted low-intensity peaks in the main decarbonation peak in the next temperature range (700-830°C). The presence of HCO_3^- explains the registered emissions of hydroxyl and carbonate ions [17, 18], while the O_2^- is related to equilibrium $CO_3^{2-} \leftrightarrow CO_2 + O^{2-}$.

The obtained results show that the equilibrium between HCO_3^-/CO_3^{2-} depends on cement components and parameters of the environment: humidity, temperature, the content of sulphur, nitrogen, carbon, gases, pH, etc. The change in the ratio of the phases containing HCO_3^-/CO_3^{2-} ions takes place at the solid-gas boundary (solid phases-atmosphere). These processes lead to changes in the chemical activity and solubility of the components of cement mortars and determine their durability, which is important for construction practice.

4th stage – an ongoing process of decarbonation and desulphurization in the temperature range 700-830°C

The decomposition of carbonate phases in the samples is carried out at a higher temperature in comparison to those of white Portland cement and marble powder (figures 2 and 3). Significant differences in mass losses were registered (3.68% for white Portland cement, 30.02% for marble powder and 29.12% for C120), because of different quantity of carbonate minerals (calcite and dolomite) in the raw materials and studied samples. The stepwise decarbonation is an indication of thermal decomposition of different carbonate-containing phases: dolomite, Mg-calcite, calcite-hydrated calcium-aluminium-carbonate silicates. Their decomposition occurs in a narrow temperature range,

resulting in splitting and intensity changes of the DTG/DSC peaks [19, 20]. The curve, describing the CO_2 release in the evolving gas analysis corresponds to the change in the DTG/DSC curves and proves the existence of overlapping thermal reactions in this stage.

4. Findings and conclusions

Traditionally, the marble powder is recognized as an inert mineral additive without taking part in processes of cement hydration. Nevertheless, this study found that the use of a marble powder addition as an aggregate and substitute for part of Portland clinker leads to:

- increasing of variety of hydrate phases;
- reducing the amount of portlandite;
- increasing the content of structurally bound water;
- densifying macro- and microstructure of mortars.

The water-to-cement ratio is an essential factor for the proper hydration of cement minerals, but also other parameters control the hydration process (quantity and pollution of mineral fillers, type and dosage of chemical admixtures, etc.). The small amounts of mass losses during the dehydration of the samples prove that studied cement-based mortars are characterised with an insufficient quantity of water for complete hydration of the cement minerals.

These results can be used to study the structure and properties of building artefacts, related to the discovery of ancient composite production technologies and environmental knowledge in various archaeological epochs.

Acknowledgements

This work was supported by the Operational Program "Science and Education for Intelligent Growth", co-financed by the European Union through the European Structural and Investment Funds under grant BG05M2OP001-1.001-0008 of National Centre for Mechatronics and Clean Technology (V.P.), by the Bulgarian Science Research Found under grant KP-06-N39/9 (V.S, B.K.) and by Laboratory of Geology - BF at NBU (B.K.).

References

[1] Aïtcin P-C 2019 *Lea's Chemistry of Cement and Concrete*, ed P Hewlett and M Liska, (Oxford: Butterworth-Heinemann) chapter 17 pp 806-820
[2] Hamad B S 1995 Investigations of chemical and physical properties of white cement concrete *Advn Cem Bas Mat* 2 161
[3] Ling T-C and Poon C-S 2011 Properties of architectural mortar prepared with recycled glass with different particle sizes *Mater. Des* 32 2675
[4] Aïtcin P-C 2007 *Binders for Durable and Sustainable Concrete* (London and New York: CRC Press) p 528
[5] Aïtcin P-C and Mindess S 2011, *Sustainability of Concrete* (Oxon and New York: CRC Press) p 328
[6] Taylor H F W 1997 *Cement Chemistry* (London: Thomas Telford Publishing) p 480
[7] EN 196-1:2016 2016 *Methods of testing cement - Part 1: Determination of strength* p 38
[8] ASTM C642-13 2013 *Standard Test Method for Density, Absorption, and Voids in Hardened Concrete* p 3
[9] Stoyanov V, Kostova B, Petkova V and Pelovski Y 2012 Structure of white cement mortars with high content of marble powder, *J Therm Anal Calorim* **110** 405
[10] Tavangarian F and Emadi R 2011 Mechanism of nanostructure bredigite formation by mechanical activation with thermal treatment, *Mater Lett*. **65** 2354
[11] Pacewska B, Wilinska I and Nowacka M 2011 Studies on the influence of different fly ashes and Portland cement on early hydration of calcium aluminate cement *J Therm Anal Calorim* **106** 859
[12] Petkova V, Stoyanov V and Pelovski Y 2012 TG–DTG–DTA in studying white self-compacting cement mortars *J Therm Anal Calorim* **109** 797

[13] Kostova B, Petkova V, Stoyanov V and Serafimova E 2016 *Proc. XV Int. Conf. on Thermal Analysis and Calorimetry in Russia (Saint-Petersburg)* vol. I (Saint-Petersburg: Peter the Great St. Petersburg Polytechnic University) p 435
[14] Olszak-Humienik M and Jablonski M 2015 Thermal behavior of natural dolomite *J Therm Anal Calorim* **119** 2239
[15] Frankeová D and Slížková Z 2016 Determination of the pozzolanic activity of mortar's components by thermal analysis, *J Therm Anal Calorim* **125**, 1115
[16] Huang Y, Wang S, Hou P, Chen Y, Gong C and Lu L 2015 Mechanisms and kinetics of the decomposition of calcium barium sulfoaluminate *J Therm Anal Calorim* **119** 1731
[17] Kamruddin M, Ajikumar P K, Dash S, Tyagi A K and Baldev R 2003 Thermogravimetry-evolved gas analysis-mass spectrometry system for materials research *Bull. Mater. Sci.* **26** 449
[18] Ghorab H Y, Zahran F S, Kamal M and Meawad A S 2018 On the durability of Portland limestone cement: Effect of pH on the thaumasite formation *HBRC Journal* **14**, 340
[19] Ximena G, Borrachero M V, Payá J, Monzó J M and Tobón J I 2018 Mineralogical evolution of cement pastes at early ages based on thermogravimetric analysis (TG), *J Therm Anal Calorim* **132** 39
[20] Djordje M, Paulin I, Kržmanc M M and Škapin S D 2018 Physical and chemical treatments influence on the thermal decomposition of a dolomite used as a foaming agent, *J Therm Anal Calorim* **131** 1125